

Joint porosity depth trend estimation and lithology/fluid classification by Bayesian inversion

Kjartan Rimstad* and Henning Omre

Department of Mathematical Sciences, Norwegian University of Science and Technology, Norway

INTRODUCTION

In this study rock physics models are used to constrain the lithology/fluid classification problem in one seismic profile without support of well observations. The rock physics models are used to establish a stochastic connection between porosity and the seismic elastic parameters. The ultimate goal of this study is to classify lithology/fluid from seismic AVO data using our stochastic depth-dependent rock physics model. The probabilistic model is considered in a Bayesian framework.

MODEL

Consider a geological model of a reservoir in one dimension, and the four classes oil-, gas- and brine-saturated sandstone, and shale. The lithology/fluid profile is denoted

$$\pi = [\pi_1, \dots, \pi_T]$$

where $\pi_i \in \{SandGas, SandOil, SandBrine, Shale\}$ and T is the number of discrete depths considered. The prior model for π is a stationary Markov chain such that

$$p(\pi) = p(\pi_T) \prod_{t=1}^{T-1} p(\pi_t | \pi_{t+1})$$

The porosity depth trends are compaction and cementation trends. The porosity, $\phi(z)$, is parametrized as in Avseth et al. (2005):

$$\begin{aligned} \phi_{Shale}(z) &= \phi_{Shale}^0 \exp\{-\alpha_{Shale}(z - z^0)\} \\ \phi_{Sand}(z) &= \begin{cases} \phi_{Sand}^0 \exp\{-\alpha_{Sand}(z - z^0)\} & \text{if } z \leq z^c \\ \phi_{Sand}(z^c) - k^c(z - z^c) & \text{if } z > z^c \end{cases} \end{aligned}$$

where ϕ_i^0 is the porosity at depth z^0 , α_i and k^c are depth trend parameters and the cementation starts at z^c , $i \in \{Sand, Shale\}$. The porosity depth trends for sand and shale are illustrated in Figure 1, where only sand has cementation. We assume that the depth z and reflection time t can be uniquely associated. All the porosity trend parameters are collected in

$$\lambda = [\phi_{Shale}^0, \phi_{Sand}^0, \alpha_{Shale}, \alpha_{Sand}, k_{Sand}^c, z_{Sand}^c]$$

and the prior model of λ is $p(\lambda)$.

We assume that seismic AVO data, d , is available. Bayesian inversion is used to determine the posterior model $p(\pi, \lambda | d)$. By using the Hertz-Mindlin model for unconsolidated rocks, and the Dvorkin-Nur contact cement model for cemented sandstones, together with Gassmann's equations for fluid effects, the connection between the seismic elastic parameters, m , and π and λ is defined. Hence the rock physics likelihood, $p(m | \pi, \lambda)$, is established. The seismic observations, d , are calculated from the seismic elastic parameters m by AVO analysis from Buland and Omre (2003), which defines the seismic likelihood $p(d | m)$. The stochastic model is summarized in Figure 2. The posterior model is hence

$$p(\pi, \lambda | d) = \text{const} \times \int p(d | m) p(m | \pi, \lambda) dm p(\pi) p(\lambda)$$

The posterior model is obtained by using a MCMC Gibbs-sampler and alternated sampling from $p(\pi | d, \lambda)$ and $p(\lambda | d, \pi)$. Gibbs-sampling from an approximation of $p(\pi | d, \lambda)$ is done efficiently by the same procedure as in Larsen et al. (2006) and λ is discretized such that we are Gibbs-sampling from a discretized $p(\lambda | d, \pi)$.

The model is applied on a synthetic case with realistic parameters and a S/N ratio of three. The true values for λ is [0.15, 0.35, 0.64, 0.1, 0.2, 2060]. The lithology/fluid profile used to generate the case together with the seismic elastic parameters and the seismic observations are plotted in Figure 3.

The prior model of the components of λ is independent normal distributions. The prior model of the Markov chain π consists of a transition matrix that has highest probability to stay in the current state, and ensure that brine never can be directly above gas or oil and only shale can be directly above gas.

RESULTS

Figure 4 illustrates the classification results. Shale and gas-saturated sandstone are mainly classified correctly, oil- and brine-saturated sandstone are more difficult to classify. We see that the classification has particular problems at depth where the differences in velocities are small, which is reasonable. The marginal posterior probability in Figure 4(b) has always positive probability for the correct class, hence the marginal posterior probability indicate all the layers.

The posterior pdf for porosity depth trend parameters are plotted in Figure 5. By comparing the prior and posterior model one observe that the algorithm manage to extract information about the ϕ^0 and z^c , but less from α and k^c . Hence for α and k^c the prior models are important for the results. Even though there are some bias in the estimates of the porosity trend parameters λ , the posterior estimates of the porosity trends itself in Figure 5(b) have small bias. Because we manage to estimate the porosity depth trend quite correctly, we also get a good estimate of the seismic elastic parameter trends for the four classes. This helps us to get better results, since we use the seismic elastic parameters in the classification.

CONCLUSION

By combining rock physics models and seismic AVO analysis a stochastic relationship between porosity depth trends/lithology and seismic observations is established. We get reasonable results if the prior models are representative. The algorithm manage to estimate the depth trend parameters and classify the lithologies in a reliable manner without any support of well observations.

The seismic data lacks the low-frequency information given by the prior background trend. We demonstrate that quantifying and reducing the uncertainty of this background trend is critical for optimal estimation and classification of lithology and fluid parameters.

The model may also easily be expanded to two or three dimensions with neighborhood dependencies. Other rock physics model and additional depth trend parameters can easily be included.

REFERENCES

Avseth, P., T. Mukerji, and G. Mavko, 2005, Quantitative seismic interpretation - applying rock physics tools to reduce interpretation risk: Cambridge University Press.
 Buland, A. and H. Omre, 2003, Bayesian linearized avo inversion: Geophysics, **68**, 185–198.
 Larsen, A. L., M. Ulvmoen, H. Omre, and A. Buland, 2006, Bayesian lithology/fluid prediction and simulation on the basis of a markov-chain prior model: Geophysics, **71**, R69–R78.

ACKNOWLEDGMENTS

The the research is part of the Uncertainty in Reservoir Evaluation (URE) activity at the Norwegian University of Science and Technology (NTNU). The support of P. Avseth and R. Holt was important for the study.

FIGURES

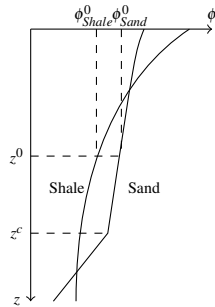


Figure 1: Porosity, ϕ , with respect to depth, z .

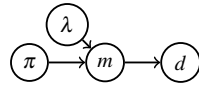


Figure 2: Stochastic model represented by a directed acyclic graph. The nodes represent stochastic variables and the arrows represent probabilistic dependencies.

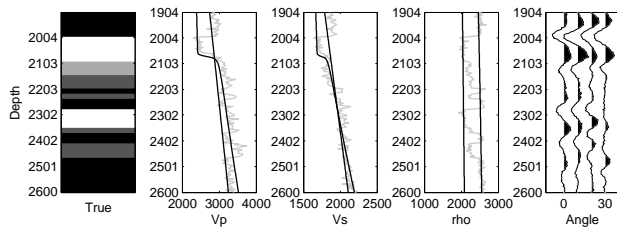
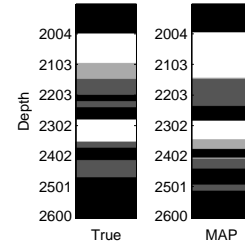
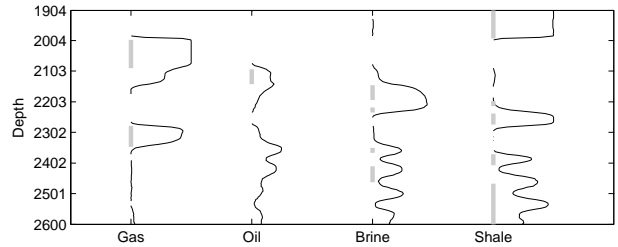


Figure 3: True lithology/fluid, seismic elastic parameter and seismic observations. Lithology/fluid: black is shale, dark gray is brine-saturated sandstone, light gray is oil-saturated sandstone and white is gas-saturated sandstone. Seismic elastic parameters in gray and black lines for trend of gas-saturated sandstone and shale calculated from the porosity trends. At 2600 the sandstone cementation begins.

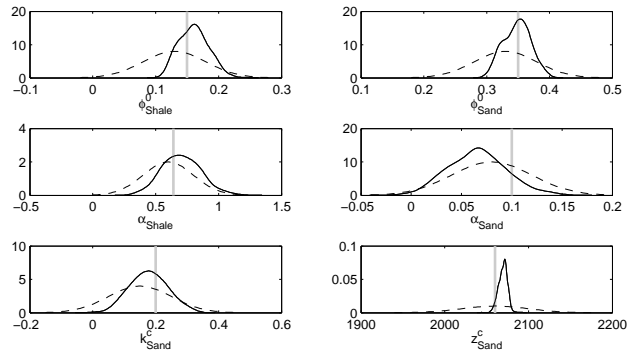


(a)

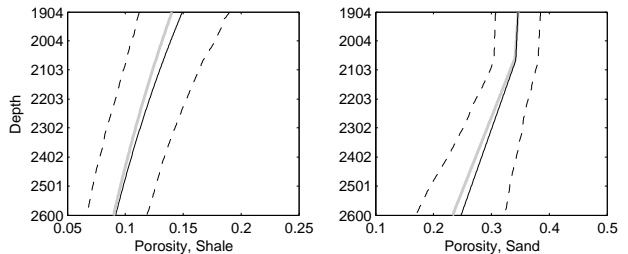


(b)

Figure 4: Lithology/fluid, $p(\pi|d)$. (a) Left plot is true case which is used to generate the seismic data, and right plot is maximum aposterior estimate (MAP). Same color code as in Figure 3 is used. (b) Gray lines indicate the true classification, and the marginal posterior probability is plotted for respectively the four classes.



(a)



(b)

Figure 5: Porosity trends, $p(\lambda|d)$. (a) Posterior pdf for the porosity trend parameters. Vertical gray lines indicate true value, dotted lines are prior models and solid lines are the posterior models. (b) Porosity trends used to generate data are in gray, and solid black lines are estimates of the porosity trend. Dotted black lines are 95% confidence bounds.